J Mater Sci: Mater Med (2008) 19:3399–3409
DOI 10.1007/s10856-008-3474-6

Silkworm and spider silk scaffolds for chondrocyte support

Kris Gellynck · Peter C. M. Verdonk · Els Van Nimmen · Karl F. Almqvist · Tom Gheysens · Gustaaf Schoukens · Lieva Van Langenhove · Paul Kiekens · Johan Mertens · Gust Verbruggen

Received: 19 January 2008 / Accepted: 15 May 2008 / Published online: 11 June 2008

Abstract *Objective* To create scaffolds with silkworm cocoon, spider egg sac and spider dragline silk fibres and examine their use for chondrocyte attachment and support. *Methods* Three different kinds of scaffolds were developed with *Bombyx mori* cocoon, *Araneus diadematus* egg sac and dragline silk fibres. The attachment of human articular cartilage cells were investigated on these bioprotein matrices. The chondrocytes produced an extracellular matrix which was studied by immunostaining. Moreover, the compression behaviour in relation to the porosity was studied. *Results* The compression modulus of a silkworm silk scaffold was related to its porosity. Chondrocytes were able to attach and to grow on the different fibres and in the scaffolds for several weeks while producing extracellular matrix products. *Conclusion* Porous scaffolds can be made out of silkworm and spider silk for cartilage regeneration. Mechanical properties are related to porosity and pore size of the construct. Cell spreading and cell expression depended on the porosity and pore-size.

K. Gellynck (✉) · E. Van Nimmen · G. Schoukens · L. Van Langenhove · P. Kiekens
Faculty of Engineering, Department of Textiles, Ghent University, Technology Park 9, 9052 Zwijnaarde, Belgium
e-mail: k.gellynck@ucl.ac.uk

P. C. M. Verdonk · K. F. Almqvist
Department of Orthopaedic Surgery, Ghent University Hospital, OK12, De Pintelaan 185, 9000 Ghent, Belgium

T. Gheysens · J. Mertens
Faculty of Sciences, Department of Biology, Terrestrial Ecology, Ghent University, K.L. Ledeganckstraat 35, 9000 Ghent, Belgium

G. Verbruggen
Department of Rheumatology, Ghent University Hospital, OK12, De Pintelaan 185, 9000 Ghent, Belgium

1 Introduction

One out of 10 patients seeking medical help for knee pain has a significant cartilage injury. Approximately 50% of these have a lesion that would benefit from, and is suitable for, surgical treatment [1]. Joint cartilage shows a very limited capacity for self-repair [2]. Advances in cell biology and tissue engineering could form a solution for this problem [3, 4].

In vitro culturing of autologous articular chondrocytes and their re-implantation in injured cartilage is already in a further clinical stage [5]. Implantation of chondrocytes for the regeneration of articular cartilage surfaces without the use of proper scaffolds has however several disadvantages [6]. As articular chondrocytes grown in vitro are injected in suspension under a periosteal flap, the function of the replaced tissue is not substituted until the cartilage is fully regenerated [7] and the dispersion of the cells or the organisation of the newly formed extracellular matrix is not controlled. Seeding the articular chondrocytes in a 3-dimensional scaffold can improve the homogeneous spreading and will support the cells until the cartilage is regenerated. The scaffold carrying the cartilage-regenerating cells can bridge the wound after implantation and help repair tissue to close the gap [8, 9].

Although many materials have been tested, the perfect biomaterial for implantation of cartilage cells has not been found yet. Most of these materials are based on polysaccharides [10]: e.g. chitosan [11] or hyaluronan [12], on gelatine [13] or on collagen or collagen/glycosaminiglycan-based constructs [14]. Non-collagen-based biomaterials used in tissue engineering scaffolds are polyglycolic acid (PGA) and polylactic acid (PLA) [15]. The most frequent problem is cellular dedifferentiation in these artificial matrices. Articular chondrocytes attached to biomaterials or encased in environments other than the original in vivo,

loose their ability to create the correct extracellular matrix when remaking cartilage. This problem might be solved using the appropriate growth factors [16].

Other problems associated with the use of scaffolds are their unsatisfied mechanical properties and rate of biodegradation. Biodegradable polymers often biodegrade too fast. PLA biodegrades after 1 or 2 months leaving not enough time for the cartilage to regenerate [17]. Ideally, the rate of biodegradation of the scaffold should not exceed the rate the newly formed repair tissue is re-established [9]. Some hydrogel-based scaffolds like alginate cannot bear enough loads to substitute the function of real cartilage [18, 19]. When the perfect scaffold would be as tough, compressible and weight-bearing as articular cartilage, the patient would be able to use his knee even before the cartilage is fully regenerated.

Recently, tissue engineering scientists have rediscovered silk as a biomaterial [20]. Silks are defined as protein polymers spun into fibres by spiders, silkworms, flies, scorpions and mites. Silk from the silkworm *Bombyx mori* is already used as suture material for centuries. However, some problems with respect to biocompatibility and allergic reactions have been reported with this type of silk. It was proven that this was due to residues of the sericin coating of these bioprotein fibres [21]. *B. mori* fibres have been tested for inflammatory responses [22, 23] and biodegradability in vitro [24]. This silk type has already been used for cell support [25] and different kinds of silk have been used as 3-dimensional scaffolds which were obtained by freeze-drying [26, 27], salt-leaching, gas-foaming [28] or in wire-rope design [29].

In contrast to *B. mori* fibres, spider silk has not been used to create scaffolds for cell support, due to its low availability.

Commercial spider silk production, as common for silkworm silk, has not succeeded yet due to the cannibalistic nature of most spiders. Kept in separate boxes, however, it is possible to breed some spiders in laboratories to obtain their egg sac and dragline silk [30, 31].

We have explored some innovative ways to create *B. mori* and *Araneus diadematus* silk scaffolds and textiles. The maintenance of the original differentiated human articular cartilage cell phenotype in these matrices or on these fibres was tested.

2 Materials and methods

2.1 *Bombyx mori* silk and the harvesting of *Araneus diadematus* silk

Three kinds of silk were used in this research. The cocoon silk from the *Bombyx mori* silkworm (SwS), the dragline (SpDS) and egg sac silk (SpESS) from the garden spider, *Araneus diadematus.*

Bombyx mori silk cocoons were kindly given by Michael Rayne (Zhejiang Cathaya International Co. Ltd., Beijing, China). By removing the sericin layer (degumming), the biocompatible sericin-free silk is obtained. The degumming was done by washing the cocoons three times in a 1% Marseille soap/0.5% Na_2CO_3 solution at 99°C during 30 min, followed by extensive rinsing with distillated water [32].

The *A. diadematus* spiders were caught in nature in Ghent during autumn and kept alive in plastic boxes by feeding them greenflies and bees. The lid of the box was covered with sandpaper or corrugated cardboard. On this rough layer the spiders could easily attach their egg sacs (Fig. 1). A pilot study proved that the biocompatibility of these SpESS fibres could be increased with enzymatic treatment: 1 mg trypsin/ml PBS at 55°C for 4 h [33].

SpDS fibres were reeled off with an in-house-made device. The legs of the spiders were kept away from their abdomen and spinnerets with a pillory-like system to prevent them from stopping the reeling (Fig. 1). Several metres of dragline silk could easily be grabbed and reeled off at a constant speed of 10 cm/s for several minutes at room temperature. Anaesthesia was not necessary and the spider was left unharmed. After the harvesting procedure the spider was released and fed. Harvested SpDS and SpESS fibres were thoroughly cleaned in distilled water prior to steam sterilization.

2.2 Preparation of the silk scaffolds

Different silk scaffolds were prepared with SwS and SpESS fibres. First of all, a non-woven based technology

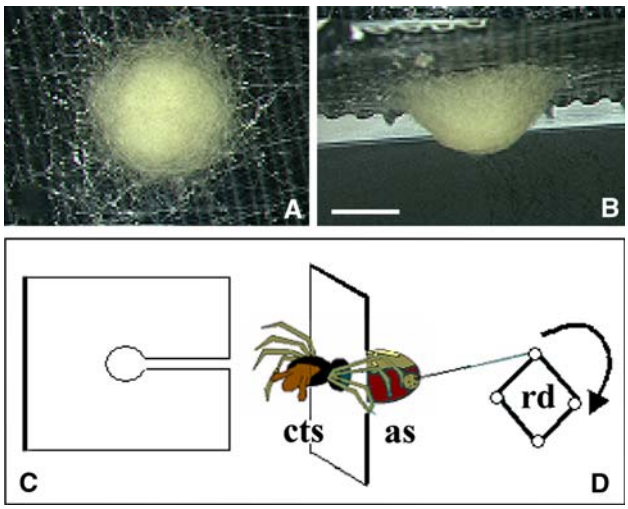

Fig. 1 (**a** and **b**) *Araneus diadematus* spider egg sac attached on corrugated cardboard; front (**a**) and side (**b**) view (scale bar 1 cm). (**c** and **d**) Pillory-like plastic construct to keep the spider legs away from the abdomen and spinnerets during dragline reeling; (**c**) pillory-like construct, front view. (**d**) Side-view, cephalothorax-side (cts) and abdomen-side (as) plus reeling device (rd)

was used to produce scaffolds keeping the native fibres intact. Furthermore, silk scaffolds with different pore sizes and porosities were regenerated with partially or completely dissolved SwS and SpESS fibres, as described below. SpDS dragline fibres were not further processed and merely analyzed for their cell support.

2.2.1 *Silk non-woven scaffolds prepared with native fibres*

These non-woven scaffolds were made with SwS and SpESS. Of 5 cm^2 rectangles were cut from a non-degummed SwS cocoon and a 2 mm spaced SwS grid was stitched on. The stitched rectangular construct was degummed afterwards. Consequently, the sericin was removed but the silkworm silk fibres were kept together in a random orientated non-woven structure consisting solely out of SwS.

In an analogous way a stitched SpESS non-woven scaffold was created. Thirty milligram of SpESS fibres were randomly put between two tissues of polyamide. The polyamide tissues under and above the SpESS fibres made it possible to stitch up an SwS yarn grid. The polyamide was then removed in formic acid (90%, 10 min), which did not harm the silk. This was tested by tensile tests performed on treated and untreated fibres (data not shown). After extensive rinsing, a SpESS non-woven composition with SwS stitches was obtained (Fig. 3).

2.2.2 *SwS fibroin regenerated scaffold by coagulation after partial dissolving*

The SwS fibres (15% w/v) were dissolved in 9 M LiBr for ½ h at 60°C. Due to the high silk concentration and the short heating time the fibres dissolved only partially. The silk/salt-mixture was highly viscous and still contained fibrils. The mixture was dialyzed subsequently against distilled water for 3–4 days. During dialysis, the silk coagulated into a clump. About 0.5 × 0.5 × 1.0 cm scaffolds were excised after the clumps had dried at room temperature for 24 h.

2.2.3 *Salt leached porous silk scaffolds using completely dissolved SwS and SpESS*

The SwS fibres were dissolved in a lower concentration (5% w/v) in 9 M LiBr for a longer period (24 h) at 60°C. Silk fibres are fully dissolved into proteins resulting in a low viscosity silk–salt mixture. Due to the lower silk concentration coagulation was avoided during dialysis over 3–4 days and an aqueous silk protein solution was acquired. This solution was freeze-dried and redissolved in 30% w/v formic acid and mixed with NaCl particles. By using NaCl particles of a particle size, 100–200 μm and 200–400 μm, the pore size of the scaffold could be controlled. The porosity was altered by changing the NaCl/silk proportions (W_{NaCl}/W_{silk}: 5/1, 10/1, 15/1). The obtained mixture was pressed in a cylindrical tube with a diameter of 8 mm. Subsequently, formic acid was evaporated at room temperature over 24 h and the mould was removed. The NaCl/silk cylinders were brought into 98% methanol for ½ h to regenerate the water insoluble silk II structure [33]. The NaCl particles were leached out in distilled water and a highly porous SwS scaffold was formed.

SpESS fibres are resistant to strong salts. Washing the SpESS fibres with the 1% Marseille soap/0.5% Na_2CO_3 soap solution, used to remove sericin from SwS fibres, whitened the SpESS fibres and diminished their resistance to strong salts. This procedure was done at 98°C during 30 min and repeated. Subsequently the fibres were dissolved in 9 M LiBr (1% w/v, 1 h, 60°C). As with SwS, the solution was dialyzed, freeze-dried, re-dissolved and blended with NaCl-particles, restructured in a methanol solution and the NaCl particles were removed to obtain a porous SpESS scaffold.

2.3 Characterization of the scaffolds

2.3.1 *Microscopic evaluation*

Next to a macroscopic evaluation, the different scaffolds (fibrous non-woven, regenerated fibrous and salt-leached porous silk scaffolds) were cross sectioned and 5-μm slices were looked at with an optical microscope (Olympus BX51, Olympus, Belgium). The scaffolds were observed with a stereo microscope (wild MS, Leica, Germany) and a scanning electron microscope (JEOL 5600 LV, JEOL, The Netherlands). A Sony 3CCD camera attached on the microscope made it possible to analyze the images with a Lucia G 4.5 imaging system.

2.3.2 *Pore interconnectivity test*

Three samples of each of the previously described silk scaffolds were brought in Indian ink for 2 h allowing the ink to migrate to the centre of the scaffold as the pores are interconnected. The scaffolds were subsequently dried and cut in two. The diffusion of the ink particles made it possible to estimate pore interconnection.

2.3.3 *Compression tests*

The compressive forces were determined on a single fibre strength tester, called the FAVIMAT (Textechno, Mönchengladbach, Germany). The FAVIMAT instrument is working according to the principle of constant rate of extension (DIN 51 221, DIN 53816, ISO 5079). It allows measuring the force at a high-resolution of 0.1 mg. Special reverse clips were mounted on the instrument in order to

convert tensile forces into compressive forces. A cross-head speed of 10 mm/min was used. The force necessary to compress the scaffold by 50% was measured.

This test was performed on the salt-leached silk scaffolds only as the porosity and the pore size was controllable for this type of scaffold. For each pore size (100–200 μm and 200–400 μm) and porosity (W_{NaCl}/W_{silk}: 5/1, 10/1, 15/1), 3 scaffolds (diameter: 0.8 mm, height: 1.5 mm, wet state) were tested.

The force necessary to compress the scaffold by 50% was measured. As W_{NaCl}/W_{silk} is proportional to the porosity of the eventual scaffold, the mechanical properties are set out against this weight-proportion to show the relation between both. An ANOVA test was performed on the results to clarify the significance of the differences.

2.4 Articular cartilage chondrocytes on silk fibres and scaffolds

2.4.1 Isolation of articular cartilage chondrocytes

Human articular chondrocytes were isolated as described elsewhere [34]. Briefly, human articular cartilage was obtained at surgery from femoral condyles of different donors. None of the donors had received corticosteroids or cytostatic drugs. Visually intact femoral condyle cartilage samples were harvested separately and prepared for culture. The cartilage samples were diced into small fragments and the chondrocytes were isolated by sequential enzymatic digestion (hyaluronidase, pronase and collagenase) of the extracellular matrix as described in detail [35]. Isolated cells were then centrifuged for 10 min at 1,500 rpm, washed three times in DMEM with 10% (v/v) FCS, tested for viability (Trypan Blue exclusion test) and counted. More than 95% of the cells were usually viable after isolation. Primary cultures of these cells were maintained in culture maximum for one week to avoid dedifferentiation before seeding. Seeding of the cells was done on three different silk-based constructs: 1—SpESS and SpDS fibres embedded in alginate gel, 2—silk non-woven constructs and 3—silk-based salt-leached scaffolds.

2.4.2 Attachment of articular chondrocytes on spider silk fibres

A 96-well culture dishes were filled with sterile agarose and kept at 6–8°C to allow the agarose to form a gel. SpESS and SpDS fibres were sterilized by autoclaving and placed on the agarose. A 0.5 ml culture medium (DMEM, 10% FCS, p/s, 60 μg/ml ascorbic acid (Sigma)) containing 1×10^6 articular chondrocytes was added to the fibres and the agarose. About 24 h of incubation at 37°C under 5% CO_2 gave the cells the time to settle on to the fibres. Subsequently, the silk was removed from the agarose with a sterile pair of tweezers. As chondocytes do not attach on agarose, only the cells attached on the silk fibres were removed. The fibres and attached cells were then drenched alternately three times into a 2% alginate-solution and a Ca^{2+}-solution. Alginate solidifies when the glucuronate and mannuronate subunits react with divalent cations such as calcium [36]. The resulting alginate gel, enclosing the fibres with the articular chondrocytes attached, was brought in culture (Fig. 2). The alginate could be removed at any time by washing the beads in 55 mM sodium citrate at a pH of 6.8 without harming the cells.

2.4.3 Seeding of articular chondrocytes on silk scaffolds and non-wovens

All silk non-wovens and silk-based scaffolds were sterilized by autoclaving before use. About 0.25 cm^2 non-wovens and 0.125 cm^3 silk scaffolds were placed in sterile 6-wells. About 1×10^6 articular chondrocytes in 0.5 ml culture medium were seeded on the silk constructs and shaken at 50 rpm during 2 h to allow the cells to spread over the pores and to enter the silk. Subsequently, culture medium was added and refreshed twice a week up to 6 weeks.

2.5 Immuno-histochemistry

After 1, 3 and 6 weeks the scaffolds were fixed in 5% formaldehyde for 24 h. The scaffold was brought in tissue freezing medium (Jung, Leica Inst., Nussloch, Germany) and a vacuum was created to make sure the freezing medium migrated in the

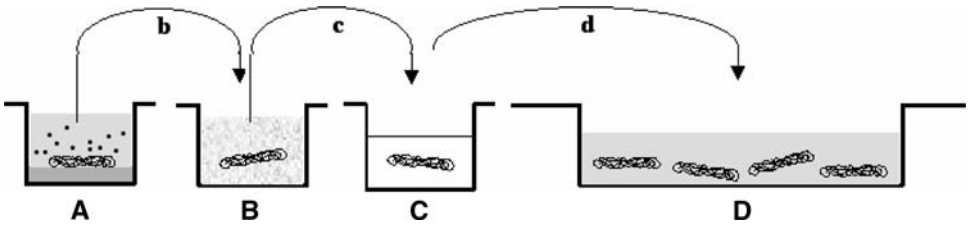

Fig. 2 Selection of chondrocytes attached on SpESS or SpDS fibres and culture of the cells/fibre constructs in alginate gel. (**a**) A 96-well culture plate with the bottom of the dishes covered with gelled agarose. Spider silk constructs are placed on the agarose and culture medium containing 1×10^6 chondrocytes is added. (**b**) After 12 h the spider silk construct with the chondrocytes attached is removed, soaked in 2% alginate and, (**c**) placed in Ca^{++} to solidify the alginate. (**d**) Chondrocytes on the spider silk constructs encased in the gelled alginate are maintained in culture in 6-well culture dishes

pores of the scaffold. After freezing (−80°C, 24 h), the entire scaffold was sliced in 5 μm slices with a cryotome (Leica CM3000; Wetzlar, Germany) to allow cell spreading to be evaluated in three dimensions. The sections were fixed in acetone/PBS. For collagen staining, the sections were brought in 50 mU/ml chondroitinase ABC (Sigma-Aldrich) in 0.1 M Tris/acetate, pH 7.6, supplemented with 1% BSA (Bovine Serum Albumine, Sigma-Aldrich). The specific ECM products were immuno-histochemically stained with an anti-type I collagen monoclonal antibody (mAb) (1 μg/ml in 0.1 M Na-fosfate buffer, pH 7.0 with 2.0% protease-free BSA; (clone I—8H5, IgG_{2a}, ICN biomedicals, Aurora, Ohio, USA)), anti-type II collagen mAb (1 μg/ml in 0.1 M Na-phosphate buffer, pH 7.0 with 2.0% protease-free BSA (clone II—4C11, IgG_1, ICN biomedicals)) and anti-aggrecan mAb (2 μg/ml in PBS pH 7.2; (clone 969D4D11, IgG_1, Biosource Europe S.A., Nivelles, Belgium)). A negative control was performed with IgG_1 isotype antibody (in PBS pH 7.2, Dakocytomation, Glostrup, Denmark). All the sections were incubated with biotinylated goat antimouse antibodies (15 min, Dakocytomation) and linked with streptavidine-peroxidase complex (horse raddisch peroxidase, Dakocytomation) for 15 min. The peroxidase-complex was coloured with AEC 'ready to use' substrate (Dakocytomation) for 10 min and the cells were then coloured in haematoxyline for 1 min.

3 Results

3.1 Characterization of the different scaffolds and non-wovens

3.1.1 Macroscopic and microscopic evaluation

As shown in Fig. 3 the shape and fibre distribution of the silk non-woven scaffolds prepared with native fibres were determined by the original morphology and arrangement of the fibres of both the *Bombyx mori* cocoon and *Araneus diadematus* egg sac. In both cases the individual fibres were homogeneously dispersed throughout the non-woven constructs. The non-woven scaffolds were 1.5 ± 0.5 mm in thickness.

Partially dissolving of the SwS fibres resulted into a highly viscous solution containing incomplete denaturated fibroin fibrils. During dialysis against pure water these fibrils conglutinated into a porous construct. By changing the parameters the physical appearance could be altered; increasing the dissolving temperature to 90°C a similar 15% (w/v) SwS sample resulted in a loss of individuality of the fibres and a more coalescent structure (Fig. 4a–d).

The SwS and SpESS salt-leached scaffolds, in which the silk fibres were completely denaturated, could be moulded in any desired shape; e.g. a cylindrical or a meniscus-shaped silk scaffold. The morphology of the SpESS-based scaffolds was not different from that of the SwS-based scaffolds. SEM-pictures and cross-sections show the difference between the fibrous pores of the partially dissolved, fibril coagulated scaffolds (Fig. 4c, d) and the pores of the salt-leached silk scaffolds (Fig. 5C–E). It is clear that in case of the salt-leached scaffolds the shape and size of the pores are driven by the shape and size of the salt particles applied. For the scaffolds based on partial dissolution of silk, the pore parameters are determined by the arrangement of the fibrils. Both kinds of silk scaffolds were more deformable in wet state and rather brittle when dried.

3.1.2 Pore interconnectivity test

The Indian ink was completely absorbed through the SwS non-wovens (Fig. 6a), in contrast to the silk fibroin regenerated scaffolds made by partially dissolving silk, where the absorption was related to the parameters used to dissolve and to dialyze the silk. An increased coalescence of the fibres and a decreasing porosity is assessed by the poor absorption of the Indian ink particles (Fig. 6b). In the salt-leached scaffolds, the Indian ink migrated through all the pores towards the centre of the construct (Fig. 6c).

3.1.3 Compression tests

The force necessary to compress the salt-leached scaffolds was inversely related to the porosity of the scaffolds. The porosity is in Fig. 7a represented by the weight proportion between silk and salt, as the pores are

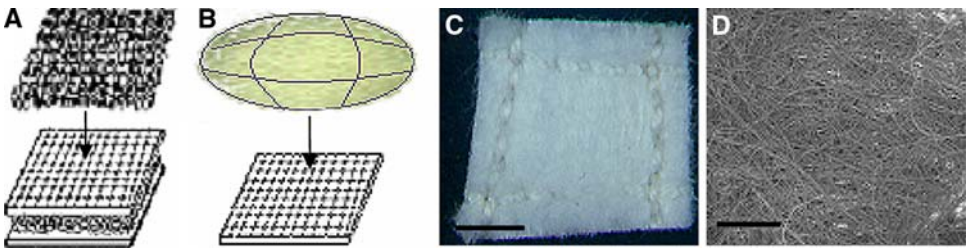

Fig. 3 Method to produce a stitched silk non-woven from (**a**) *Araneus diadematus* egg sac and from (**b**) *Bombyx mori* cocoon between polyamide tissues. (**c**) A *B. mori* silk non-woven with a stitched silk yarn grid (scale bar: 5 mm). (**d**) SEM magnification of the individual fibres in the silk non-woven (scale bar: 500 μ)

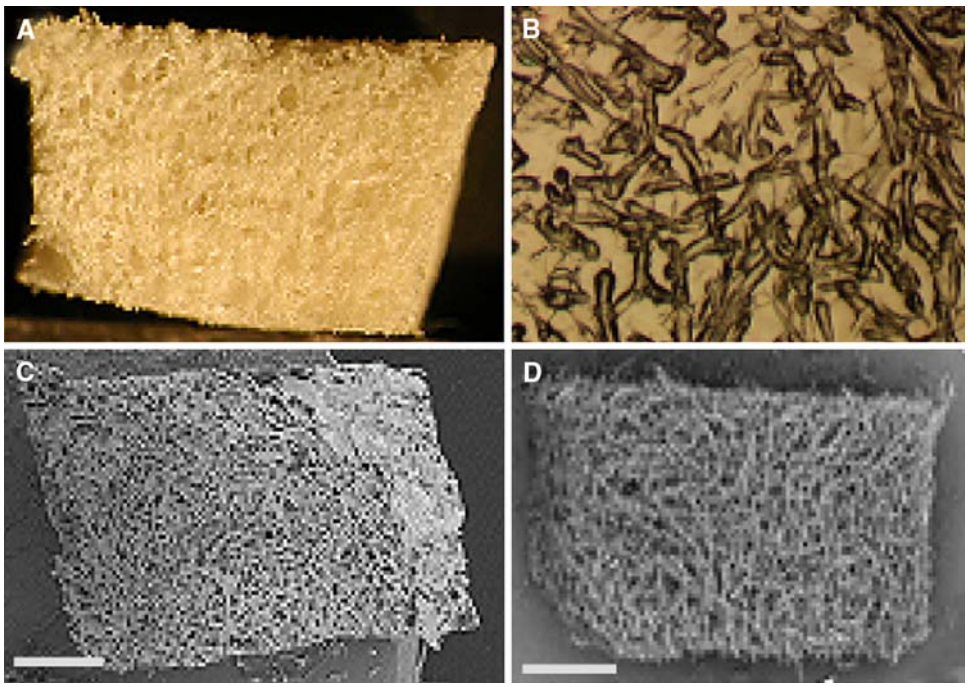

Fig. 4 Partially dissolved and coagulated scaffolds. (**a**) Stereomicroscope (**b**) light microscope: cross section showing fibrillar structure. SEM-pictures showing silk materials dissolved at (**c**) 90°C and (**d**) 60°C. Scale bars: 100 nm

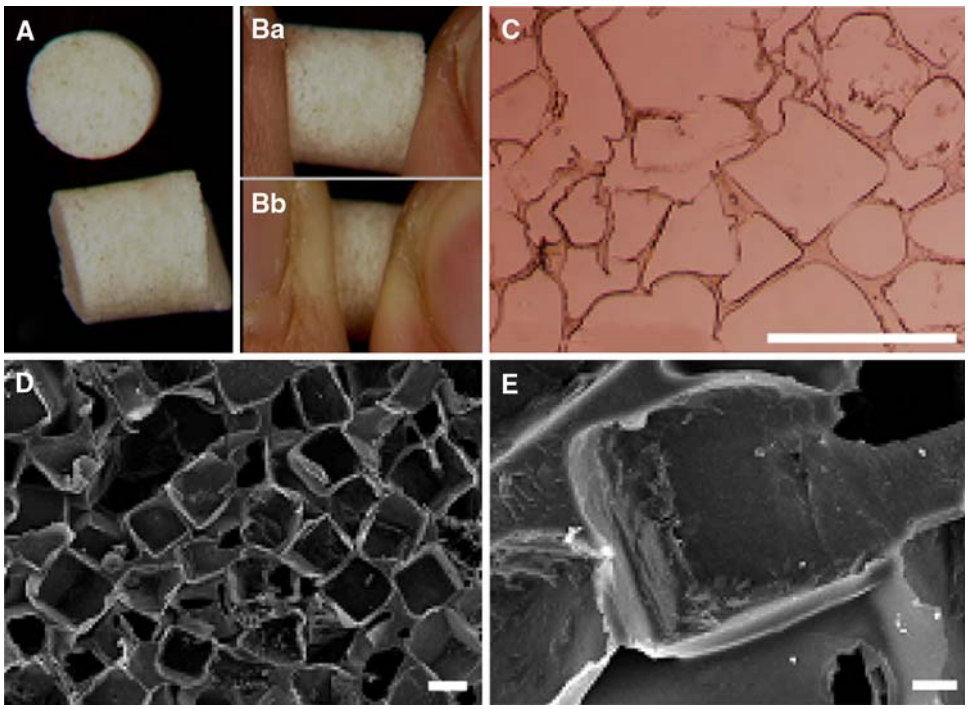

Fig. 5 (**A**) Salt-leached silkworm silk scaffolds. (**B**) Macroscopic picture of uncompressed (**a**) and compressed (**b**) salt-leached scaffold (**C**) light microscopy, cross section of silk scaffold, space bar: 500 μm. (**D**) SEM-picture ×100, space bar 100 nm (**E**) SEM-picture ×600, space bar 20 nm

Fig. 6 Ink absorption in (**a**) silk non-woven structure, (**b**) three different partially dissolved silk scaffolds and in (**c**) salt-leached scaffold

made by the salt particles. With the same porosity, scaffolds with higher number of smaller pores needed 18.67, 18.02 and 20.91% more compressive strength for the same strain than those with a smaller number of larger pores, e.g. samples resulting from salt/silk proportion of 5, 10 and 15, respectively. Since, based on a two factor ANOVA, the interaction between pore size and salt/silk proportion was found to be significant ($P < 0.001$), the two factors were combined into one

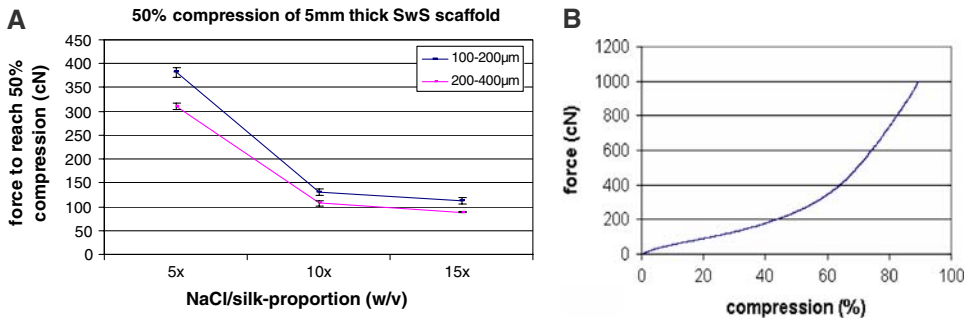

Fig. 7 (**a**) Relation between the forces needed to reach 50% compression and the pore size and the silk/salt proportion of the SwS salt-leached silk scaffolds. The silk/salt proportion is directly related to the porosity as the washed out salt particles are forming the pores. The test was performed on three scaffolds for each pore size and salt–silk proportion. (**b**) stress–compression curve up till 90% of one SwS salt-leached silk scaffold

factor. Together with the compression values, a one-way ANOVA was performed, in combination with the Scheffé-test for "Comparisons of means". For a salt/silk proportion of 5/1, there is a significant difference between the results for 100–200 µm and for 200–400 µm ($P < 0.001$). For higher salt/silk proportion, there is still a significant difference between the different pore sizes, however much smaller ($0.01 < P < 0.05$). With respect to the effect of salt/silk proportion, there is no significant difference between the results for a salt/silk proportion of 10/1 and 15/1 ($P > 0.05$).

The force needed to compress the SwS scaffold and SpESS scaffolds with the same pore-size (100–200 µm) and porosity (silk/salt 10% w/w) did not differ significantly ($P > 0.05$): SwS scaffold: 25.62 ± 2.10 kPa, SpESS: 24.11 ± 1.56. One stress-compression curve up to 90% compression is shown in Fig. 7b.

3.2 Interaction of articular cartilage chondrocytes with silk fibre/scaffold

3.2.1 Articular chondrocyte anchorage on SpESS and SpDS embedded in alginate

Articular chondrocytes attached to the SpESS and SpDS fibres and embedded in alginate, could be observed through the alginate with the light microscope. Cells were attached on the fibres and some clusters of cells were formed around the fibres (Fig. 8a). When the alginate was dissolved, the silk fibres and their attached articular chondrocytes could be examined more in detail (Fig. 8b, c). On both SpESS and SpDS fibres large amounts of attached cells could be retrieved after several weeks of culture.

3.2.2 Articular chondrocytes cultured in the silk non-woven constructs

The cells seeded on the silk non-wovens could be observed attached on and around the silk fibres up to 6 weeks after seeding. The articular chondrocytes on the non-wovens were not homogeneously dispersed, but found in groups. However, the cells could be found all over the fabric. Immuno-histochemistry showed the presence of type I and II collagen and, to a lesser extent, also aggrecan (Fig. 9).

3.2.3 Articular chondrocytes cultured in the silk-based salt-leached scaffolds

The migration of cells in the partially dissolved silk scaffolds varied from one scaffold to another. In some of these scaffolds, articular chondrocytes were only found in the outer regions of the scaffold, whereas in others, cells could be found in every cross-section. The uneven dispersal of the cells did not allow exact cell numbers to be quantified on the histological sections. However, the control of pore size and porosity of the salt-leached silk scaffolds offered a method to keep cell migration under control. When the 200–400 µm salt particles were used, the cells scattered

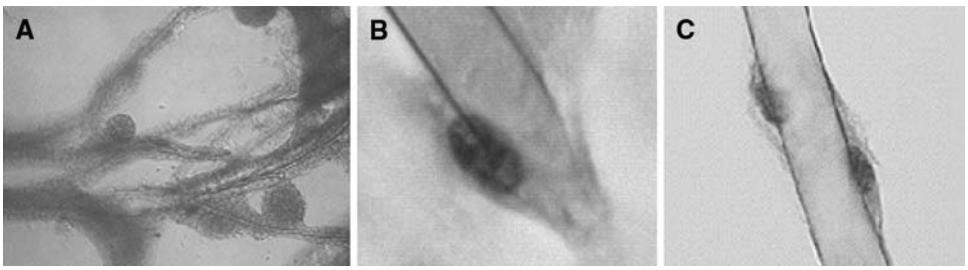

Fig. 8 (**a**) Articular chondrocytes around and clustered on SpESS embedded in alginate. (**b**, **c**) Details of a chondrocyte on SpESS and on SpDS fibre, respectively

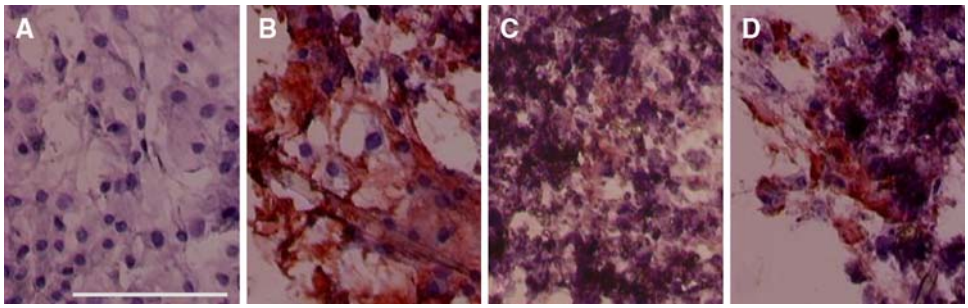

Fig. 9 Chondrocyte expression of extracellular matrix constituents in a SwS non-woven. (**a**) control, (**b**) type I collagen, (**c**) type II collagen, (**d**) aggrecan. Space bar: 100 μm

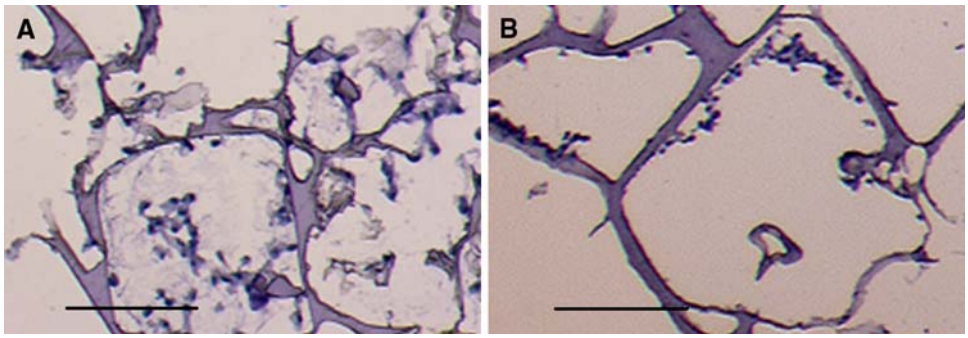

Fig. 10 Chondrocytes growing in salt-leached silk scaffolds. (**a**) small pores 100–200 μm; cells with extracellular matrix are filling up the pores, but are captured within several pores. (**b**) large pores 200–400 μm; cells remain attached on the walls of the pores. Space bar: 100 μm

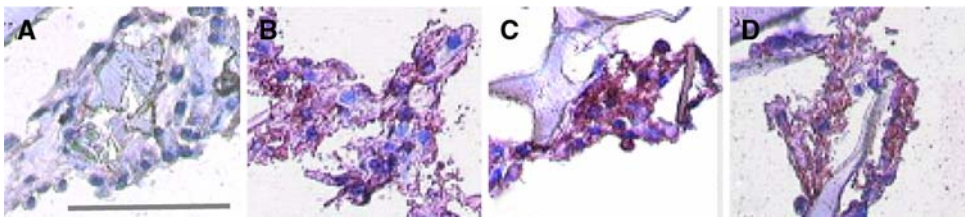

Fig. 11 Chondrocyte expression of extracellular matrix constituents in a salt-leached silk scaffold. (**a**) control, (**b**) type I collagen, (**c**) type II collagen, (**d**) aggrecan. Space bar: 100 μm

over the whole scaffold and were present in most of the pores. Cells in these larger pores remained attached to the sides and could not fill the pore with cell and ECM-material. In the smaller pore scaffolds (100–200 μm salt particles) the cells were captured within a few pores**.** Chondrocytes growing in smaller pores filled up the whole pore with ECM. The typical ovoid, chondrocyte-like shape was still present after 6 weeks of culture in the scaffolds, exemplifying the differentiated phenotype of the cells in culture (Fig. 10). Type I and II collagen and aggrecan were detected in all the samples around the cells. However, staining for type II collagen and aggrecan was more intense than for type I collagen (Fig. 11).

4 Discussion

Silkworm silk is commercially used as a yarn in woven textiles; the fibre is too expensive to be used in non-wovens for non-medical purposes. The method described shows that small scale production of a silk non-woven construct or scaffold is achievable. Therefore, an original method to harvest spider draglines and egg sacs from *Araneus diadematus* without harming the spiders has been developed. Like this, anaesthesia or taping of the spiders was avoided [37]. Non-woven spider and silkworm silk fibre constructs can then be made from both steam-sterilized *Bombyx mori* cocoons and *A. diadematus* egg sacs without harming the fibres and their mechanical properties [38]. In these cases the individual cleansed and sterilized fibres were homogeneously dispersed throughout our novel non-woven construct which were 1.5 ± 0.5 mm in thickness and on which articular cartilage cells were easily seeded (Fig. 3).

Silk, partially or completely dissolved in strong salts [24], can be further processed as a polymer. Removal of the salts from the solution induced a slow self-assembly process of the incompletely denaturated fibroin fibrils to form a porous construct. This event was accelerated with methanol to regenerate the insoluble silk II structure [39]. Although, spider silk appeared tougher to dissolve than silkworm silk, porous scaffolds could be made with spider egg sac silk fibres as well. Increasing the dissolving temperature to 90°C for instance resulted in a loss of individuality of the SwS fibres and a more coalescent structure.

Using the methods described, porous SwS and SpESS salt-leached silk scaffolds with any desired shape, porosity and pore size were created. Contrary to SwS-based salt-leached silk scaffolds [28], the manufacture and use of SpESS salt-leached silk scaffolds for biological use have not been described in literature. The morphology of the SpESS-based scaffolds was not different from that of the SwS-based scaffolds.

The Indian ink tests did demonstrate the interconnectivity of the pores. The ink particles were completely absorbed through the SwS non-wovens, in contrast to the silk fibroin regenerated scaffolds, where an increased coalescence of the fibres and a decreasing porosity resulted in a poor absorption of the Indian ink. In the salt-leached scaffolds, the ink migrated through all the pores towards the centre of the construct. There was a clear relation between the absorption of the ink and the cell migration in the scaffolds. Mechanical testing revealed that forces necessary to compress the salt-leached scaffolds were inversely related to the porosity of the scaffolds. The experimental design thus resulted in the creation of spider and silkworm derived scaffolds allowing variable degrees of cell invasion and different physical characteristics.

The results reported in the alginate-embedding method described show that articular chondrocytes are able to attach and to grow on SpESS and SpDS fibres embedded in alginate. After embedding in alginate the cells were maintained in culture up to 3 weeks. Articular cartilage cells have been shown to retain their original articular cartilage chondrocyte phenotype when cultured in alginate gel [40]. When these cells had been anchored on the fibres and were embedded in alginate, the preservation of the ovoid cell shape by cartilage cells expressing anchorage-dependent growth on the fibrous material is noteworthy. This finding provides evidence that these spider silk fibres are not cytotoxic and can be used for cell support in biomaterials.

Chondrocytes that had attached on the salt-leached scaffolds still showed the typical articular cartilage cell ovoid shape after 6 weeks of culturing. Cell division and extracellular matrix expression did not differ between SpESS and SwS fibre-based scaffolds. Attached on all silk surfaces, the articular chondrocytes expressed type II collagen and aggrecan, although type I collagen was detected with the immunostaining also. The presence of type I collagen was suggestive of some degree of transdifferentiation of the implanted chondrocytes. This transdifferentiation has been observed in more in vitro culture systems and might have been resulted from specific interaction with the material the cells anchored on, or to the lack of growth factors and compressive stimuli [16, 41].

The development of spider silk-based materials with different physical properties, e.g. well-defined resistances against tensile and compressive stresses, should enable their use in different bioengineered tissues.

The advantage of the non-woven towards the other scaffolds is that the silk fibres have not been denatured and still keep their original mechanical properties, i.e. their resistance against tensile stresses. Therefore, these fibres could be used as biomaterials in sutures, and in matrices for tendon or ligament regeneration. Conversely, the salt-leached silk scaffolds adequately resist compressive strength. The compressive properties between SpESS and SWS-based scaffolds did not differ significantly. However, the resistance of these salt-leached silk scaffolds against mechanical forces is far beyond the one of unharmed silk fibres. This inconvenience can be solved by armoring the salt-leached silk scaffolds with silk fibres. Using dragline silk fibres as reinforcement, the mechanical properties of draglines and of porous silk scaffolds can be combined. Such materials could be used in cartilage implant procedures. In cartilage tissue, resistance to compressive stress is determined by the proteoglycans of the extracellular matrix and the resistance against tensile forces is ascertained by the collagen framework. This way, the combination of silk fibres and salt-leached scaffold may provide a candidate material mimicking cartilage tissue.

To avoid stress shielding of an implanted salt-leached silk-based scaffold, the compression modulus of the latter should be less than that of cartilage [38]. The force necessary to compress the salt-leached silk scaffolds was dependent on the pore size and porosity, but in all cases lower than for cartilage [42]. Furthermore, the elastic nature of the scaffolds was illustrated when they reverted to their original shape immediately after the compressive force was released.

As a conclusion, the biomedical potential of silkworm and spider silk can be anticipated from their mechanical properties [23] and slow biodegradability [24]. These protein fibres are not cytotoxic as cells can adhere and grow thereon for several weeks. The different silk fibres can be processed in non-woven and porous scaffolds, in which human articular chondrocytes can migrate, culture and express their typical extracellular matrix products. As these porous scaffolds can be made in any shape and reinforced with fibres with appropriate mechanical properties, these can be used in tissue engineering applications such as cartilage, meniscus, tendon and ligament regeneration.

Acknowledgement This project was funded by the BOF (Special research Fund: B/03191/01, fund IV1) of the University of Ghent, and by FWO Grant 3G026305.

References

1. A. Aroen, S. Loken, S. Heir, E. Alvik, A. Ekeland, O.G. Granlund, Articular cartilage lesions in 993 consecutive knee arthroscopies. Am. J. Sports Med. **32**, 211–215 (2004)

2. J.A. Buckwalter, H.J. Mankin, Articular cartilage: degeneration and osteoarthritis, repair, regeneration, and transplantation. Instr. Course Lect. **47**, 487–504 (1998)
3. E.B. Hunziker, Articular cartilage repair: basic science and clinical progress. A review of the current status and prospects. Osteoarthr. Cartilage **10**, 432–463 (2002)
4. L.A. Solchaga, V.M. Goldberg, A.I. Caplan, Cartilage regeneration using principles of tissue engineering. Clin. Orthop. **391**(Suppl), S161–S170 (2001)
5. L. Peterson, T. Minas, M. Brittberg, A. Nilsson, E. Sjogren-Jansson, A. Lindahl, Two- to 9-year outcome after autologous chondrocyte transplantation of the knee. Clin. Orthop. Relat. Res. **374**, 212–234 (2000)
6. M. Brittberg, L. Peterson, E. Sjogren-Jansson, T. Tallheden, A. Lindahl, Articular cartilage engineering with autologous chondrocyte transplantation. A review of recent developments. J. Bone Joint Surg. Am. **85**(A Suppl 3), 109–115 (2003)
7. A. Ferruzzi, P. Calderoni, B. Grigolo, G. Gualtieri, Autologous articular chondrocytes implantation: indications and results in the treatment of articular cartilage lesions of the knee. Chir. Organi. Mov. **89**, 125–134 (2004)
8. R.D. Coutts, R.M. Healey, R. Ostrander, R.L. Sah, R. Goomer, D. Amiel, Matrices for cartilage repair. Clin. Orthop. **391**(Suppl), S271–S279 (2001)
9. L. Lu, X. Zhu, R.G. Valenzuela, B.L. Currier, M.J. Yaszemski, Biodegradable polymer scaffolds for cartilage tissue engineering. Clin. Orthop. **391**(Suppl), S251–S270 (2001)
10. L. Galois, A.M. Freyria, L. Grossin, P. Hubert, D. Mainard, D. Herbage, J.F. Stoltz, P. Netter, E. Dellacherie, E. Payan, Cartilage repair: surgical techniques and tissue engineering using polysaccharide- and collagen-based biomaterials. Biorheology **41**, 433–443 (2004)
11. A. Subramanian, H.Y. Lin, D. Vu, G. Larsen, Synthesis and evaluation of scaffolds prepared from chitosan fibres for potential use in cartilage tissue engineering. Biomed. Sci. Instrum. **40**, 117–122 (2004)
12. D.L. Nettles, T.P. Vail, M.T. Morgan, M.W. Grinstaff, L.A. Setton, Photocrosslinkable hyaluronan as a scaffold for articular cartilage repair. Ann. Biomed. Eng. **32**, 391–397 (2004)
13. W. Xia, W. Liu, L. Cui, Y. Liu, W. Zhong, D. Liu, J. Wu, K. Chua, Y. Cao, Tissue engineering of cartilage with the use of chitosan-gelatin complex scaffolds. J. Biomed. Mater. Res. **15**, 373–380 (2004)
14. N. Veilleux, M. Spector, Effects of FGF-2 and IGF-1 on adult canine articular articular chondrocytes in type II collagen-glycosaminoglycan scaffolds in vitro. Osteoarthr. Cartilage **13**, 278–286 (2005)
15. Z. Ma, C. Gao, Y. Gong, J. Shen, Cartilage tissue engineering PLLA scaffold with surface immobilized collagen and basic fibroblast growth factor. Biomaterials **26**, 1253–1259 (2005)
16. P.M. van der Kraan, P. Buma, T. van Kuppevelt, W.B. van den Berg, Interaction of articular chondrocytes, extracellular matrix and growth factors: relevance for articular cartilage tissue engineering. Osteoarthr. Cartilage **10**, 631–637 (2002)
17. J.M. Moran, D. Pazzano, L.J. Bonassar, Characterization of polylactic acid-polyglycolic acid composites for cartilage tissue engineering. Tissue Eng. **9**, 63–70 (2003)
18. K.F. Almqvist, L. Wang, J. Wang, D. Baeten, M. Cornelissen, R. Verdonk, E.M. Veys, G. Verbruggen, Culture of articular chondrocytes in alginate surrounded by fibrin gel: characteristics of the cells over a period of eight weeks. Ann. Rheum. Dis. **60**, 781–790 (2001)
19. S. Hsu, S. Wen Whu, S. Hsieh, C. Tsai, D. Chanhen Chen, T. Tan, Evaluation of chitosan-alginate-hyaluronate complexes modified by an RGD-containing protein as tissue-engineering scaffolds for cartilage regeneration. Artif. Organs **28**, 693–703 (2004)
20. G.H. Altman, R.L. Horan, H.H. Lu, J. Moreau, I. Martin, J.C. Richmond, D.L. Kaplan, Silk matrix for tissue engineered anterior cruciate ligaments. Biomaterials **23**, 4131–4141 (2002)
21. C.M. Wen, S.T. Ye, L.X. Zhou, Y. Yu, Silk-induced asthma in children: a report of 64 cases. Ann. Allergy **65**, 375–378 (1990)
22. M. Santin, A. Motta, G. Freddi, M. Cannas, In vitro evaluation of the inflammatory potential of the silk fibroin. J. Biomed. Mater. Res. **46**, 382–389 (1999)
23. B. Panilaitis, G.H. Altman, J. Chen, H.J. Jin, V. Karageorgiou, D.L. Kaplan, Macrophage responses to silk. Biomaterials **24**, 3079–3085 (2003)
24. R.L. Horan, K. Antle, A.L. Collette, Y. Wang, J. Huang, J.E. Moreau, V. Volloch, D.L. Kaplan, G.H. Altman, In vitro degradation of silk fibroin. Biomaterials **26**, 3385–3393 (2005)
25. N. Minoura, S. Aiba, Y. Gotoh, M. Tsukada, Y. Imai, Attachment and growth of cultured fibroblast cells on silk protein matrices. J. Biomed. Mater. Res. **29**, 1215–1221 (1995)
26. M.Z. Li, S.Z. Lu, Z.Y. Wu, Study on porous silk fibroin materials 1: fine structure of freeze-dried silk fibroin. J. Appl. Polym. Sci. **79**, 2185–2191 (2001)
27. M.Z. Li, Z. Wu, C. Zhang, S. Lu, H. Yan, D. Huang, H. Ye, Study on porous silk fibroin materials II. Preparation and characteristics of spongy porous silk fibroin materials. J. Appl. Polym. Sci. **79**, 2192–2199 (2001)
28. R. Nazarov, H.J. Jin, D.L. Kaplan, Porous 3-D scaffolds from regenerated silk fibroin. Biomacromolecules **5**, 718–726 (2004)
29. U.J. Kim, J. Park, H.J. Kim, M. Wada, D.L. Kaplan, Three-dimensional aqueous-derived biomaterial scaffolds from silk fibroin. Biomaterials **26**, 2775–2785 (2005)
30. F. Vollrath, Biology of spider silk. Int. J. Biol. Macromol. **24**, 81–88 (1999)
31. (a) F. Vollrath, Strength and structure of spiders' silks. J. Biotechnol. **74**, 67–83 (2000); (b) E. Servoli, D. Maniglio, A. Motta, R. Predazzer, C. Migliaresi, Surface properties of silk fibroin films and their interaction with fibroblasts. Macromol. Biosci. **5**(12), 1175–1183 (2005)
32. M. Tsukada, G. Freddi, P. Monti, A. Bertoluzza, N. Kasai, Structure and molecular conformation opf Tussah silk fibroin films: effect of methanol. J. Polym. Sci. **33**, 1995–2001 (1995)
33. K. Gellynck, P. Verdonk, R. Forsyth, K.F. Almqvist, E. Van Nimmen, T. Gheysens, L. Van Langenhove, P. Kiekens, J. Mertens, G. Verbruggen, Biocompatibility and biodegradability of spider egg sac silk. J. Mater. Sci. Mater. Med. (2008, in press)
34. M. Cornelissen, G. Verbruggen, A.M. Malfait, E.M. Veys, C. Broddelez, L. De Ridder, The study of representative populations of native aggrecan aggregates synthesized by human chondrocytes in vitro. J. Tiss. Cult. Meth. **15**, 139–146 (1993)
35. L. Wang, G. Verbruggen, K.F. Almqvist, D. Elewaut, C. Broddelez, E.M. Veys, Flow cytometric analysis of the human articular chondrocyte phenotype. Osteoarthr. Cartilage **9**, 73–84 (2001)
36. C. Sartori, D.S. Finch, B. Ralph, K. Gilding, Determination of the cation content of alginate thin films by FTIR spectroscopy. Polymer **38**, 43–51 (1997)
37. C. Riekel, B. Madsen, D. Knight, F. Vollrath, X-ray diffraction on spider silk during controlled extrusion under a synchrotron radiation X-ray beam. Biomacromolecules **1**, 622–626 (2000)
38. E. Van Nimmen, K. Gellynck, D. De Bakker, T. Gheysens, J. Mertens, P. Kiekens, L. Van Langenhove, Research and development of spider silk for biomedical applications. in *Proceedings SEM Annual Conference on Experimental and Applied Mechanics, Biological Inspired and multi-Functional Materials and Systems; Milwaukee*, Wisconsin, USA, 10–12 June 2002

39. C. Dicko, D. Knight, J.M. Kenney, F. Vollrath, Conformational polymorphism, stability and aggregation in spider dragline silks proteins. Int. J. Biol. Macromol. **36**(4), 215–224 (2005)
40. H. Liu, Y.W. Lee, M.F. Dean, Re-expression of differentiated proteoglycan phenotype by dedifferentiated human chondrocytes during culture in alginate beads. Biochim. Biophys. Acta **1425**(3), 505–515 (1998)
41. C.J. Hunter, J.K. Mouw, M.E. Levenston, Dynamic compression of chondrocyte-seeded fibrin gels: effects on matrix accumulation and mechanical stiffness. Osteoarthr. Cartilage **12**, 117–130 (2004)
42. P.A. Hardy, A.C. Ridler, C.B. Chiarot, D.B. Plewes, R.M. Henkelman, Imaging articular cartilage under compression—cartilage elastography. Magn. Reson. Med. **53**(5), 1065–1073 (2005)